Journal of Integrative Neuroscience

J. Integr. Neurosci. **2022**; 21(2): 070
https://doi.org/10.31083/j.jin2102070

Original Research

Morphometric and volumetric analysis of the posterior cranial fossa in adult Chiari malformation type I with and without group B basilar invagination

Yongzhi Xia[1], Haijian Xia[1], Wei Tang[1], Shengxi Wang[1], Yi Yan[1,*]

[1]Department of Neurosurgery, The First Affiliated Hospital of Chongqing Medical University, 400016 Yuzhong District, Chongqing, China
*Correspondence: yiyan@hospital.cqmu.edu.cn (Yi Yan)
Academic Editor: Rafael Franco
Submitted: 16 November 2021 Revised: 19 December 2021 Accepted: 31 December 2021 Published: 23 March 2022

Abstract

Background: The frequent association of basilar invagination (BI) makes the understanding of the pathogenesis of Chiari malformation type I (CMI) difficult. The influence of group B type of BI (the BI without obvious atlantoaxial instability) on the skeletal morphology has not been thoroughly studied. The objective of this study is to evaluate the skeletal alterations in the posterior cranial fossa (PCF) of adult CMI cases with and without group B BI. **Methods**: Fifty-four adult CMI without BI cases (CMI-only group) and 30 adult CMI with group B BI cases (CMI-BI group) were retrospectively studied. Fifty-six adult patients with unruptured intracranial aneurysms were included as the controls. Several linear and angular variables, and the bony volume of the PCF were analyzed based on thin-slice computed tomography data. **Results**: Morphological analysis revealed a significant difference in several variables from controls compared to CMI-only, and CMI-BI patients. The clivus and occipital bone, shortened and elevated in CMI-only patients, were further flattened in BI-associated CMI patients. Furthermore, although out of the scope for the diagnostic threshold of BI, the CMI-only cases also had a tendency to form BI. The association of BI modified several variables, without further reducing the bony PCF volume. **Conclusions**: These findings indicate that the variables associated with group B BI tend to be a continuum of the same pathological abnormalities that originate from the same pathological alterations in CMI patients.

Keywords: Basilar invagination; Chiari malformation type I; Computer tomography; Foramen magnum decompression; Posterior cranial fossa

1. Introduction

Chiari malformation and basilar invagination (BI) are common malformations of the craniocervical junction (CVJ) in adults [1]. BI is defined as the invagination of the high cervical spine into the cranial base [1–4]. Chiari malformation type I (CMI) is characterized by the caudal herniation of the cerebellar tonsils through the foramen magnum into the spinal canal [2,4–6].

BI may also result in CMI in some patients [7,8]. Each of these two clinical entities can be present individually, but they frequently occur synchronously [1,4,9,10]. The term "CMI" was used in previous studies, without excluding BI-associated cases, which limits our knowledge regarding the pathogenesis of the underlying CMI [11]. Goel divided BI into two groups, based on the presence (group A) or absence (group B) of the instability of the atlantoaxial region, as demonstrated by an abnormal increase in the atlanto-dental interval [12] (Fig. 1). Due to the differences in the pathogenesis, manifestation and treatment [10], the group A BI-associated CMI cases were excluded from this study.

It is generally believed that CMI patients tend to have reduced volume in the posterior cranial fossa (PCF) [2,6,13]. Our previous study confirmed decreased bony PCF volume in simple CMI cases without BI or atlantoaxial dislocation [14]. Despite numerous studies, the origin and pathophysiology of CMI, especially the subset combined with BI, remains controversial [15–19]. A thorough comparative analysis of the skeletal structures of the PCF in simple CMI and BI-associated CMI cases has not been reported [10]. The objective of this study was to evaluate the differences of the CVJ skeleton in CMI with and without BI, based on data derived from thin-slice computer tomography (CT).

2. Materials and methods

2.1 Patient population

We retrospectively studied 120 adult CMI cases who had received foramen magnum decompression (FMD) in the Neurosurgical Department of the First Affiliated Hospital of Chongqing Medical University from January 2015 to April 2020. CMI cases with or without group B type of BI were designated as the CMI-BI group or CMI-only group, respectively. Cases combined with atlantoaxial instability were diagnosed as atlantoaxial dislocation (AAD), and excluded from this study. Gender and age matched patients with un-ruptured intracranial aneurysms were included as the controls. The control cases underwent regular CT angiography, to eliminate the inclusion of patients with BI

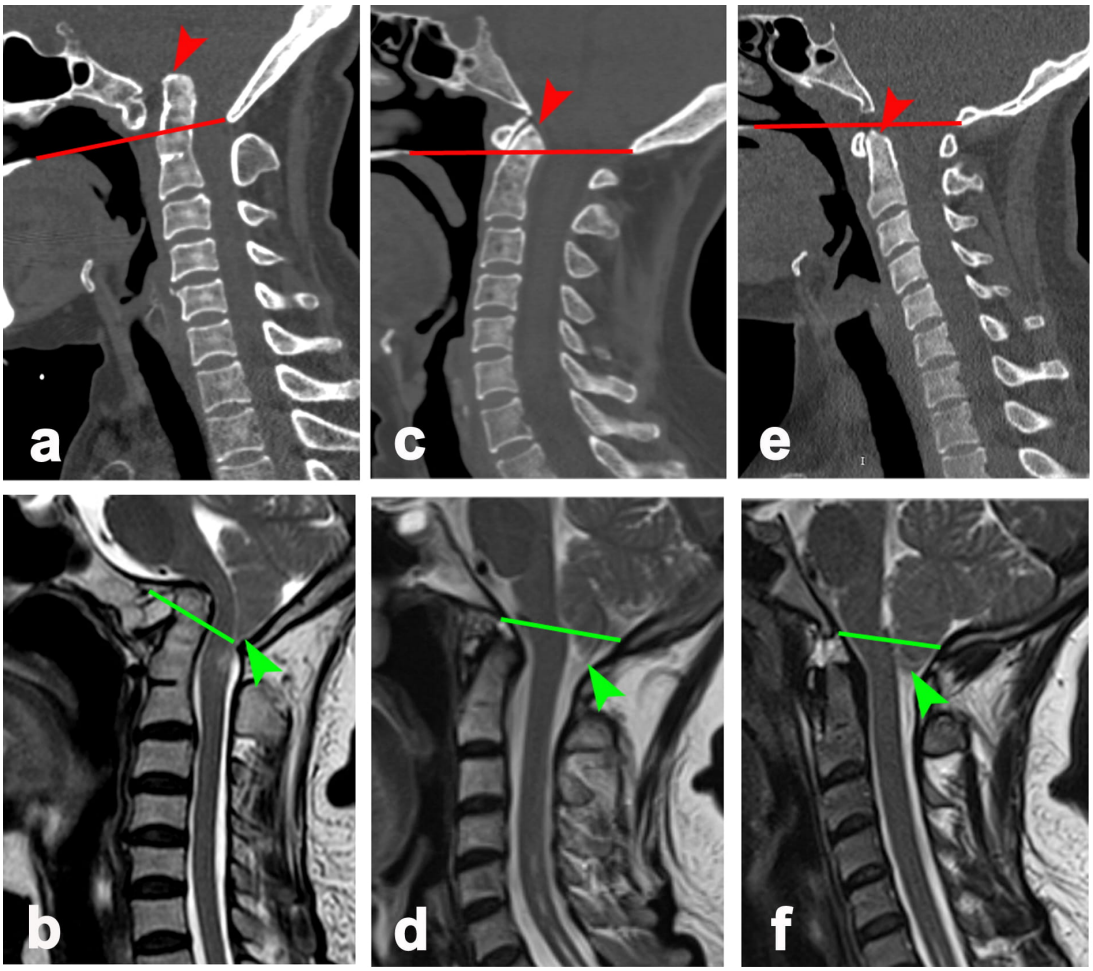

Fig. 1. The reconstructed mid-sagittal CT and MRI T2-WI image of three types of craniocervical junction malformation. (a,b) CMI with Group A BI. (c,d) CMI with Group B BI. (e,f) CMI without BI. Red line, the Chamberlain line; Red arrow, the tip of dens; Green line, the McRae line; Green arrow, the tip of herniated cerebellar tonsil.

or AAD. An informed consent of all participants was obtained. All procedures performed in studies involving human participants were approved by the Ethics Committee of the First Affiliated Hospital of Chongqing Medical University.

The diagnostic criteria for CMI was defined as the presence of cerebellar tonsils which protruded through the foramen magnum by more than 5 mm in the sagittal MRI T2 image (Fig. 1). BI was diagnosed if the tip of the dens was more than 5 mm above Chamberlain's line in the reconstructed mid-sagittal CT image (Fig. 1). AAD was diagnosed if the atlanto-dental interval was more than 3 mm on CT, or in the presence of instability which was confirmed on dynamic X-rays of the CVJ. The inclusion criteria were as following: (1) a diagnosis of CMI; (2) patients older than 18 years. The exclusion criteria were: (1) cases associated with AAD (group A BI), or other bone malformations in the CVJ; (2) cases with acquired cerebellar tonsil herniation; (3) cases with other spinal cord malformations, such as the tethered cord syndrome; (4) cases associated with spine surgery or trauma.

2.2 Radiological evaluation

CT scans (0.6 mm each slice) were obtained for each CMI patient, with the neck in a neutral position, on a 128-slice multi-detector CT scanner (Siemens, Germany). The images in DICOM format were reconstructed in three orthogonal planes using RadiAnt DICOM Viewer, version 5.5.0. (Medixant, Poland) software. The images of the control group obtained from the CT angiography were also analyzed using the same methods. Eight linear and 9 angular parameters (Table 1) were measured on the mid-sagittal image, according to our previous method [14] (Fig. 2), using RadiAnt or iPhotoDraw V2.6 software (Simen Wu, Canada). The first author evaluated all of the exams to minimize variations in measurements.

The volume of the bony PCF was calculated using Mimics Research, version 18.0.0.525 (Materialise NV, Leuven, Belgium), according to a previous method [14]. Briefly, a mask was constructed to define the bony boundary in the axial, sagittal and coronary planes, and the tool of region growing was used to reconstruct a 3-D model. Thus,

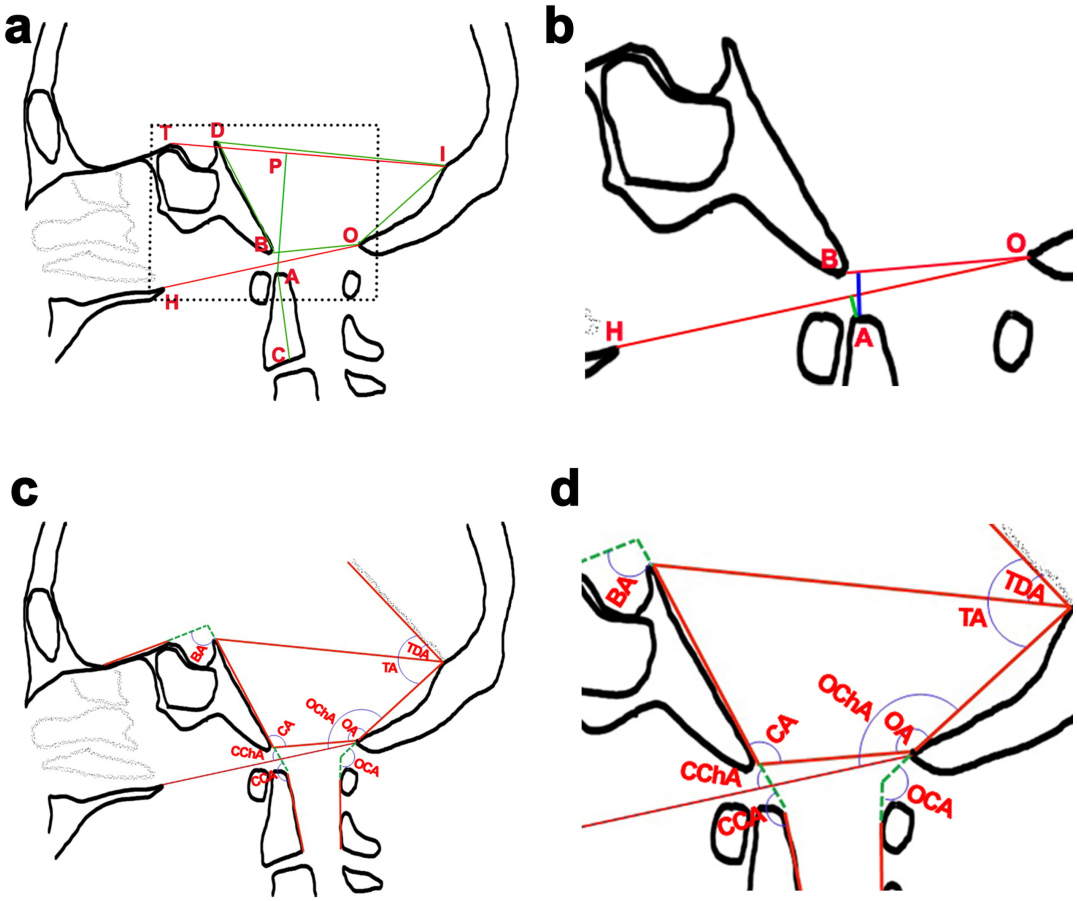

Fig. 2. Diagrams showing the linear and angular measurements on a mid-sagittal image. (a,b) Chamberlain's line (HO), McRae line (BO), clivus length or CL (DB), Supraoccipital length or SOL (IO), anterio-posterior length of PCF or AP-PCF (DI), Klaus height index or KHI (PA), axial length or AL (AC). b, magnification of the dashed rectangle in a. The green line, Violation of the Chamberlain's line (VC); the blue line, Violation of the McRae line (VM). A, the tip of the dens; B, basion; C, midpoint of the inferior endplate of C2 vertebrae; D, top of the dorsum dorsum; H, posterior margin of the hard palate; I, internal occipital protuberance; P, the point on the line of TI shortest to the tip dens axis; O, opisthion; T, tuberculum sellae. (c,d) BA, basal angle; CA, clivus angle; CAA, clivus axial angle; CChA, clivus Chamberlain's line angle; OA, occipital angle; OCA, occipital cannal angle; OChA, occipital Chamberlain's line angle; TA, tentorial angle; TDA, tentorial dorsum sellae angle. d, local magnification of c.

the volume of the bony PCF was calculated automatically (Fig. 3).

2.3 Statistical analysis

IBM SPSS 19.0 software (IBM Corp., Armonk, NY, USA) was used for statistical analysis. The descriptive statistics are presented as the means, standard deviations, ranges, and 95% confidence intervals (CIs). The adherence chi-squared test was used to analyze the difference in gender. The value of VM, CL, AP-PCF, KHI, BA, CChA, CAA, OCA, TA and TDA were compared using parametric ANONA. The age, VC, AL, ML, SOL, CA, OA and OChA were compared using Kruska-Wallis tests and subsequent peer evaluation. Measures of multiple linear correlation were obtained between several variables, using Spearman to evaluate the possible associative inferences. Statistically significance was indicated by a p-value < 0.05.

3. Results

Of the 120 CMI cases, 36 were excluded due to missing or incomplete images. Finally, 54, 30 and 56 cases were included in CMI-only, CMI-BI and control group, respectively.

There were 41 females and 11 males in CMI-only group, with a mean age of 46.63 $\pm$ 10.72 years (range 18–64 years); 16 females and 14 males in CMI-BI group, with a mean age of 46.07 $\pm$ 12.04 years (range 18–69 years); 35 females and 21 males in the control group, with a mean age of 48.04 $\pm$ 10.96 years (range 21–75 years). There were no differences between 3 groups in age ($p = 0.578$) and gender (chi-square test: $p = 0.091$).

All CMI patients presented with neurological symptoms, including neuropathic pain, limb numbness, sensory disturbance, muscle weakness and ataxia. Seventy-six pa-

Table 1. Abbreviation list of the linear and angular measurements.

Abbreviation	Full form	Definition
Linear measurements		
AL	axial length	distance from the midpoint of the inferior margin of axis to the tip of dens
AP-PCF	anteroposterior diameter of posterior cranial fossa	distance from the center of the internal occipital protuberance to the dorsum sellae
CL	clivus length	distance between the top of the dorsum sellae and the basion
KHI	Klaus height index	the vertical line from the dens tip to the line between internal occipital protuberance and the tuberculum sellae
ML	McRae line	distance from the opisthion to basion
SOL	supraoccipital length	distance from the center of the internal occipital protuberance to the opisthion
VC	violation of the Chamberlain's line	distance from the tip of dens above the line extending from the palate to the opisthion
VM	violation of the McRae line	distance from the tip of dens above the line extending from basion to the opisthion
Angular measurements		
BA	basal angle	angle measured from the base of the anterior cranial fossa and a line drawn between the top of the dorsum sellae and the basion
CA	clivus angle	angle formed by the MaRae line and the line along the inferior half of the clivus
CAA	clivus axial angle	angle formed by a line along the posterior margin of the dens and the line along the inferior half of the clivus
CChA	clivus Chamberlain's line angle	angle measured by a line drawn along the inferior half of the clivus and the Chamberlain's line
OA	occipital angle	angle formed by the line of SOL and the McRae line
OCA	occipital canal angle	angle formed by the SOL and the line along the posterior wall of the C1-2 canal
OChA	occipital Chamberlain's line angle	angle formed by the SOL and the Chamberlain's line
TA	tentorial angle	angle formed by the tentorium and the line of SOL
TDA	tentorial dorsum sellae angle	angle formed by the tentorium and the line from the dorsum sellae to the internal occipital protuberance

The values of VC and VM were recorded as negative when the dens tip was below the corresponding line.

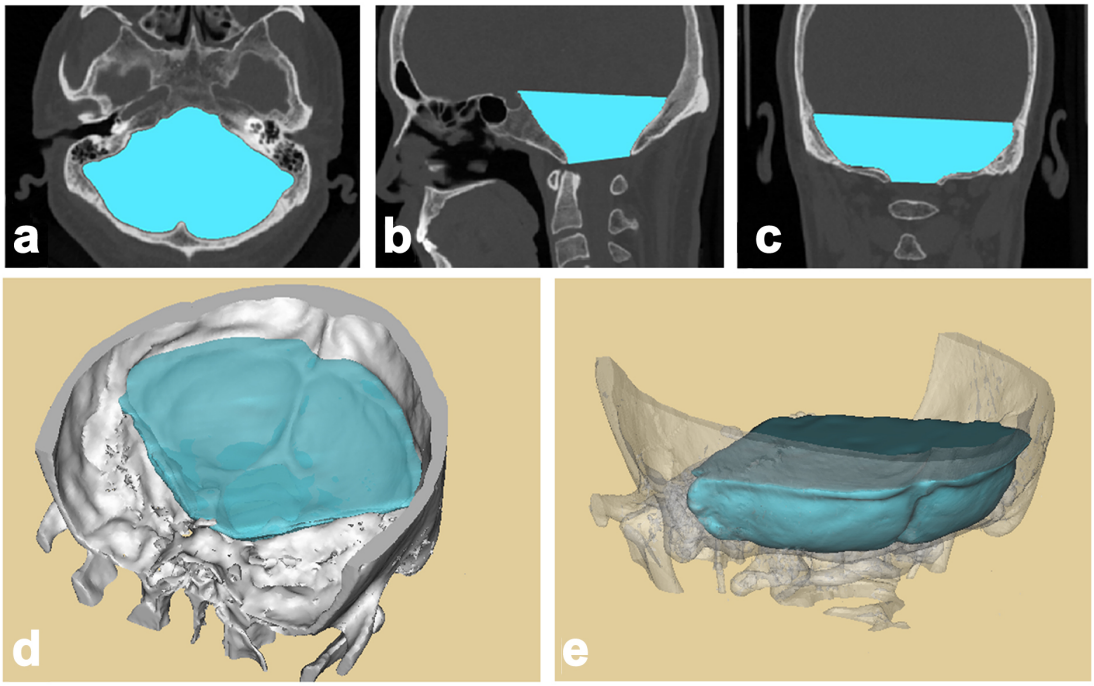

Fig. 3. Illustration of the measurement of the bony PCF using Mimics Research software. A mask was constructed to define the bony boundary in axial (a), sagittal (b) and coronary image (c), and a 3D model (d,e) was reconstructed using the tool of region growing in Mimics.

tients (90.48%; 49 cases in CMI-only group, and 27 cases in CMI-BI group) had syringomyelia.

3.1 Linear measurements

Results of linear measurements are summarized in Table 2.

(a) VC and KHI. The VC increased, and KHI diminished progressively from the control to CMI-only, and CMI-BI group, with significant differences ($p < 0.05$).

(b) VM. VM of CMI-BI patients were significantly larger than the control ($p = 0.000$) and CMI-only group ($p = 0.000$), however, no significant differences were observed between the control and CMI-only group ($p = 0.546$).

(c) CL, SOL and AL. CL, SOL and AL in CMI-BI ($p = 0.000$, $p = 0.011$, and $p = 0.007$) and CMI-only group ($p = 0.000$, $p = 0.000$, and $p = 0.000$) were significantly smaller than those in the control, however no significant differences were observed between the two CMI groups ($p = 0.063$, $p = 0.269$, and $p = 0.926$).

(d) ML and AP-PCF. No significant differences were observed between either of these 3 groups ($p > 0.05$).

3.2 Angular measurements

Results of angular measurements are summarized in Table 2.

(a) BA, CChA, CA and CAA. BA and CA increased progressively from the control to CMI-only ($p = 0.001$, $p = 0.000$), and CMI-BI group ($p = 0.027$, $p = 0.000$). While, CChA and CAA diminished progressively from the control group to CMI-only ($p = 0.000$, $p = 0.000$), and CMI-BI group ($p = 0.000$, $p = 0.000$).

(b) OChA. The value of OChA in CMI-BI ($p = 0.015$) and CMI-only group ($p = 0.001$) was significantly larger than the control, but there was no significant difference between the two CMI groups ($p = 0.897$).

(c) OA. OA in CMI-BI group was significantly smaller than the CMI-only group ($p = 0.000$) and the control ($p = 0.000$). There was no significant difference between CMI-only and the control group ($p = 0.324$).

(d) OCA and TA. OCA and TA in CMI-BI group were significantly larger than the control ($p = 0.036$, $p = 0.039$). No significant differences were observed in the CMI-only group when compared with CMI-BI ($p = 0.289$, $p = 1.000$) and the control group ($p = 0.867$, $p = 0.081$).

(e) TDA. No significant differences were observed between either of these 3 groups ($p > 0.05$).

3.3 Volumes of bony PCF

The volumes of bony PCF in CMI-BI ($p = 0.000$) and the CMI-only group ($p = 0.000$) were significantly decreased than the control, but there was no significant difference between the two CMI groups ($p = 0.943$) (Table 2).

3.4 Correlations between major variables

Correlations were calculated among the major variables. Mild and moderate correlations were obtained. The findings are summarized in Table 3.

4. Discussion

Our research studied the skeletal alterations in the PCF of CMI cases associated with and without BI, and confirmed that the association of BI aggravates the invagination of the clivus and occipital bones of the CMI, without further reducing the volume of the bony PCF. Furthermore, although not diagnosed as BI, according to the threshold of 5 mm, the CMI-only cases also had a tendency to form BI.

CMI is defined as the herniation of the cerebellar tonsil by more than 5 mm below the foramen magnum [2,4–6]. However, this simplistic definition masks the complex nature of this heterogeneous abnormality [20]. The etiology and pathogenesis of CMI still remain poorly defined since its initial description [2,21]. The theory of a developmentally reduced PCF is not applicable in all CMI cases. Therefore, the conclusions from different studies have varied considerably [2,5,11,19,22–28]. Most studies have supported a smaller PCF in adult CMI [5,11,23–26], while others reported no difference [19,27,28]. Furthermore, nearly all studies failed to exclude BI-associated cases [5,11,19,23–28]. Recently, we reported that simple CMI, associated without BI and AAD, presents with a reduced bony PCF volume [14].

BI is defined as the violation of Chamberlain's line by the odontoid process of the axis. The limit of 5.0 mm is most frequently used for the diagnosis [4]. BI can be divided into two groups, according to the presence (group A) or absence (group B) of obvious atlantoaxial instability [12]. Since the etiology, pathogenesis, and treatment are largely different, our study examined only group B BI-associated cases, which usually present without foramen magnum invasion [12]. As BI is diagnosed based on the skeletal abnormality, theoretically the PCF volume of the BI-associated CMI cases may also be affected.

Although they are frequently found simultaneously, CMI and BI can present independently [1,4,9,10]. The pathogenesis of CMI with BI remains controversial [15–18]. This study found that all CMI cases, with or without BI, present with decreased bony PCF volume. Surprisingly, the association of BI did modify some linear and angular parameters of the PCF, but not the bony PCF volume of CMI.

All the decreased linear dimensions (AL, CL and SOL) are measurements in the rostral-caudal direction. It may be concluded that the hypoplasia of the clivus and occipital bone may be the cause of these morphological changes, although the three parameters were not further reduced in the BI-associated cases. Since the ML and AP-PCF remained unchanged, the value of CL and SOL may have affected the PCF volume, which was demonstrated by the moderate correlations in Table 3. This analysis revealed

Table 2. The linear, angular and volumetric results in the 3 groups.

Parameters	Control	CMI-only	CMI-BI
	($\bar{x} \pm s$)	($\bar{x} \pm s$)	($\bar{x} \pm s$)
	(95% CI L to U)	(95% CI L to U)	(95% CI L to U)
Linear measurements			
VC (mm)	–0.66 ± 3.23	1.16 ± 3.02 ***	8.54 ± 4.45***#
	(–1.54 to 0.22)	(0.34 to 1.99)	(6.88 to 10.20)
KHI (cm)	3.97 ± 0.46	3.38 ± 0.39 ***	2.78 ± 0.43 ***###
	(3.85 to 4.10)	(3.28 to 3.49)	(2.62 to 2.94)
CL (cm)	4.49 ± 0.39	4.15 ± 0.33 ***	3.96 ± 0.31 ***
	(4.39 to 4.60)	(4.06 to 4.24)	(3.84 to 4.08)
SOL (cm)	4.28 ± 0.45	3.82 ± 0.49 ***	3.97 ± 0.55 *
	(4.16 to 4.40)	(3.70 to 3.96)	(3.76 to 4.17)
AL (cm)	3.35 ± 0.28	3.15 ± 0.22 ***	3.15 ± 0.25 **
	(3.27 to 3.43)	(3.09 to 3.21)	(3.06 to 3.24)
VM (mm)	–4.96 ± 1.59	–4.59 ± 1.29	–2.81 ± 1.44 ###***
	(–5.39 to –4.54)	(–4.94 to –4.24)	(–3.35 to –2.27)
ML (cm)	3.47 ± 0.25	3.38 ± 0.24	3.55 ± 0.59
	(3.41 to 3.54)	(3.32 to 3.45)	(3.33 to 3.77)
AP–PCF (cm)	8.28 ± 0.48	8.27 ± 0.53	8.47 ± 0.49
	(8.15 to 8.41)	(8.12 to 8.41)	(8.29 to 8.65)
	(118.68 to 122.37)	(126.16 to 130.63)	(140.82 to 148.25)
Angular measurements			
BA (º)	108.24 ± 6.45	113.00 ± 6.71 (51) **	117.26 ± 7.81***#
	(106.51 to 109.96)	(111.11 to 114.89)	(114.23 to 120.29)
CChA (º)	67.49 ± 3.85	63.32 ± 5.08 (53) ***	57.46 ± 6.65 (29) ***###
	(66.45 to 68.53)	(61.92 to 64.73)	(54.93 to 59.99)
CA (º)	120.52 ± 6.88	128.39 ± 8.19 ***	144.54 ± 9.96 ***###
CAA (º)	158.87 ± 8.65	150.87 ± 6.88 ***	139.59 ± 10.26 ***###
	(156.48 to 161.25)	(149.00 to 152.75)	(135.76 to 143.42)
OChA (º)	135.21 ± 6.25	140.29 ± 8.59 (53) **	139.74 ± 9.59*
	(133.52 to 136.89)	(137.91 to 142.67)	(136.02 to 143.46)
OA (º)	128.17 ± 6.81	129.03 ± 7.85	118.91 ± 12.43***###
	(126.35 to 130.00)	(126.88 to 131.17)	(114.27 to 123.56)
OCA (º)	136.79 ± 10.44	139.34 ± 11.51	144.00 ± 16.27 *
	(133.88 to 139.69)	(136.20 to 142.48)	(137.93 to 150.08)
TA (º)	97.64 ± 8.03	94.04 ± 8.30 (46)	92.87 ± 7.78*
	(95.49 to 99.79)	(91.58 to 96.51)	(89.79 to 95.95)
TDA(º)	41.48 ± 6.55	40.95 ± 7.03	39.05 ± 5.12
	(39.73 to 43.24)	(38.86 to 43.03)	(37.02 to 41.08)
Volumetric measurements			
PCF volume (mL)	159.58 ± 18.26	138.10 ± 20.80 ***	142.44 ± 16.09 ***
	(154.69 to 164.47)	(132.42 to 143.77)	(136.43 to 148.44)

Compared with Control: *, $p < 0.05$; **, $p < 0.01$; ***, $p < 0.001$. Compared with CMI-only: #, $p < 0.05$; ###, $p < 0.001$.

a difference in several variables in the 3 groups, including VC, KHI, BA, CA, CChA and CAA. The VC and KHI reflect the degree of the dens prolapsing towards the posterior cranial base, which indicates that CMI-only cases also have a tendency to form BI, even though these alterations are not significant enough for these CMI cases to be diagnosed as BI. The CA and CAA reflect the degree of ventral compression to the brainstem. These changes may result from the shortening and flattening of the clivus. The inclination of the tentorium and the shape of the occipital bone may modify the values of TA and TDA. As the TDA remains stable, the flattening of the occipital bone may exist in the BI-associated cases.

The FMD was reported as the cornerstone of the treatment strategy for CMI [2,15,29]. A greater increase in the postoperative PCF volume has been associated with a greater likelihood of clinical improvements in CMI patients [30–32]. Larger increases in the caudal portion of the PCF

Table 3. Spearman correlations between variables.

	CL	SOL	KHI	CA	CAA	CChA	BA	PCF volume
VC	$R = –0.545$	$R = –0.022$	R = –0.749	$R = 0.829$	$R = –0.522$	$R = –0.527$	$R = 0.316$	$R = –0.184$
	$p = 0.000$	$p = 0.796$	$p = 0.000$	$p = 0.000$	$p = 0.000$	$p = 0.000$	$p = 0.000$	$p = 0.030$
CL	$R = 1.000$	$R = 0.183$	$R = 0.679$	$R = –0.599$	$R = 0.317$	$R = 0.399$	$R = –0.409$	$R = 0.417$
	$p = 0.000$	$p = 0.000$	$p = 0.000$	$p = 0.000$	$p = 0.000$	$p = 0.000$	$p = 0.000$	$p = 0.000$
SOL	$R = 0.183$	$R = 1.000$	$R = 0.331$	$R = –0.079$	$R = 0.155$	$R = 0.112$	$R = –0.203$	$R = 0.540$
	$p = 0.000$	$p = 0.000$	$p = 0.000$	$p = 0.353$	$p = 0.070$	$p = 0.051$	$p = 0.018$	$p = 0.000$
KHI	$R = 0.679$	$R = 0.331$	$R = 1.000$	$R = –0.776$	$R = 0.556$	$R = 0.558$	$R = –0.472$	$R = 0.431$
	$p = 0.000$	$p = 0.000$	$p = 0.000$	$p = 0.000$	$p = 0.000$	$p = 0.000$	$p = 0.000$	$p = 0.000$
CA	$R = –0.599$	$R = –0.079$	$R = –0.776$	$R = 1.000$	$R = –0.599$	$R = –0.746$	$R = 0.452$	$R = –0.254$
	$p = 0.000$	$p = 0.353$	$p = 0.000$	$p = 0.000$	$p = 0.000$	$p = 0.000$	$p = 0.000$	$p = 0.002$
CAA	$R = 0.317$	$R = 0.155$	$R = 0.556$	$R = –0.599$	$R = 1.000$	$R = 0.617$	$R = –0.508$	$R = 0.219$
	$p = 0.000$	$p = 0.070$	$p = 0.000$	$p = 0.000$	$p = 0.000$	$p = 0.000$	$p = 0.000$	$p = 0.010$
CChA	$R = 0.399$	$R = 0.112$	$R = 0.558$	$R = –0.746$	$R = 0.617$	$R = 1.000$	$R = 0.190$	$R = 0.266$
	$p = 0.000$	$p = 0.051$	$p = 0.000$	$p = 0.000$	$p = 0.000$	$p = 0.000$	$p = 0.001$	$p = 0.000$
BA	$R = –0.409$	$R = –0.409$	$R = –0.472$	$R = 0.452$	$R = –0.508$	$R = 0.190$	$R = 1.000$	$R = –0.275$
	$p = 0.000$	$p = 0.000$	$p = 0.000$	$p = 0.000$	$p = 0.000$	$p = 0.001$	$p = 0.000$	$p = 0.001$
PCF volume	$R = 0.417$	$R = 0.540$	$R = 0.431$	$R = –0.254$	$R = 0.219$	$R = 0.266$	$R = –0.275$	$R = 1.000$
	$p = 0.000$	$p = 0.000$	$p = 0.000$	$p = 0.002$	$p = 0.010$	$p = 0.000$	$p = 0.001$	$p = 0.000$

volume are also associated with a greater likelihood of improvement in syrinx and cervicomedullary kinking [30]. BI is a significant predictor of poor outcomes in CMI after FMD [33]. Since CMI-BI patients present without further reduction in the bony PCF volume, the size of FMD may not be the only factor that determines the prognosis. Effective decompression of the brain stem is determined not only by the size of the FMD, but also the resection of the posterior arch of the atlas, the performance of a duraplasty, and tonsil resection. A relatively larger size of FMD to further increase the caudal portion of the PCF volume, might be a potential treatment for these patients [34]. However, the optimal patient-specific PCF volume increase is difficult to determine, and might be better predicted on the basis of the individual preoperative neuroimaging. Our study suggests that FMD size could be tailored to the individual PCF volume in CMI patients. However, in some CMI cases with severe BI (present with larger CA and smaller CCA), the FMD is not enough to relieve the ventral compression to the brainstem. Odontoidectomy may be a better choice for these special cases [17].

This study confirmed that the pathophysiology of both CMI and group B BI involves hypoplasia of the skull at the CVJ region, especially the clivus and the occipital bone. Our findings suggest that the hypoplasia of the clivus and occipital bones underlie the pathologies of CMI, and that CMI cases without BI also have a tendency to form BI. The association of BI may aggravate the flattening, rather than the reduction, of the clivus and occipital bone. Together, it indicates that BI may be a continuum of the same pathological phenomenon that originates from the same pathological alterations seen in CMI patients.

The authors are not aware of any other study that attempted to elucidate the role of group B type of BI in the morphology of CMI. There are several limitations with this study. 89% of the cases in our series were associated with syringomyelia, higher than the 20–72% in previous reports [5]. Since syringomyelia is usually secondary to tonsillar herniation, and syringomyelia formation is irrelevant to the PCF volume [35], these differences should not affect our conclusions. Secondly, CT images may be more difficult to show the tentorium in all slices, compared to MRI [14], so the bony PCF in this study does not include the upper part of the total PCF under the tentorium. An evaluation based on MRI may provide more information on the total PCF volume. Due to the discrepancy in races, districts and gender, further studies are needed to better understand the morphological changes of CMI in patients with various backgrounds and ethnicities.

5. Conclusions

Our study indicates that CMI exhibits hypoplasia in both the occipital bone and the clivus, and the tendency to form BI. The association of BI further aggravates the hypoplasia of these bones, by invagination of the posterior cranial fossa base, without further reduction of the length of the clivus, the occipital bone, and the bony PCF volume. This suggests that Group B BI may be a continuum of the same pathological phenomenon that originates from the same pathological alterations in CMI. These results provide new insights into skeletal change in CMI, which may help to further understand the pathogenesis of CMI.

Abbreviations

AAD, atlantoaxial dislocation; AL, axial length; AP-PCF, anteroposterior diameter of the posterior cranial fossa;

BA, basal angle; BI, basilar invagination; CA, clivus angle; CAA, clivus axial angle; CL, clivus length; CMI, Chiari malformation type I; CVJ, craniocervical junction; Dis-Cham, distance between the dens tip and the Chamberlain line; Dis-McRae, distance between dens tip and the McRae line; FMD, foramen magnum decompression; KHI, Klaus height index; ML, McRae line; OA, occipital angle; OCA, occipital canal angle; PCF, posterior cranial fossa; SOL, supraoccipital length; TA, tentorial angle; TDA, tentorial dorsum sellae angle; VC, violation of the Chamberlain's line. VM, violation of the McRae line.

Author contributions

YZX and YY conceived and designed the experiments; SXW and YZX collected and analyzed the data; HJX and WT reviewed and validated the data; YZX wrote the paper.

Ethics approval and consent to participate

An informed consent of all participants were obtained. All procedures performed in studies involving human participants were approved by the institutional research committee of the First Affiliated Hospital of Chongqing Medical University (No. 2020-315).

Acknowledgment

We thank Wenyuan Tang of the First Affiliated Hospital of Chongqing Medical University for excellent criticism of the article.

Funding

This study was supported by grants from the science and health joint project of Chongqing City (No. 2020FYYX233) and the subject cultivation project of the First Affiliated Hospital of Chongqing Medical University.

Conflict of interest

The authors declare no conflict of interest.

References

[1] Goel A. Basilar invagination, Chiari malformation, syringomyelia: a review. Neurology India. 2009; 57: 235.

[2] Bolognese PA, Brodbelt A, Bloom AB, Kula RW. Chiari I Malformation: Opinions on Diagnostic Trends and Controversies from a Panel of 63 International Experts. World Neurosurgery. 2019; 130: e9–e16.

[3] Botelho RV, Ferreira EDZ. Angular craniometry in craniocervical junction malformation. Neurosurgical Review. 2013; 36: 603–10; discussion 610.

[4] Klekamp J. Chiari I malformation with and without basilar invagination: a comparative study. Neurosurgical Focus. 2015; 38: E12.

[5] Alkoç OA, Songur A, Eser O, Toktas M, Gönül Y, Esi E, *et al*. Stereological and Morphometric Analysis of MRI Chiari Malformation Type-1. Journal of Korean Neurosurgical Society. 2015; 58: 454–461.

[6] Aydin S, Hanimoglu H, Tanriverdi T, Yentur E, Kaynar MY. Chiari type I malformations in adults: a morphometric analysis of the posterior cranial fossa. Surgical Neurology. 2005; 64: 237–41; discussion 241.

[7] Goel A. Is atlantoaxial instability the cause of Chiari malformation? Outcome analysis of 65 patients treated by atlantoaxial fixation. Journal of Neurosurgery. Spine. 2015; 22: 116–127.

[8] Behari S, Kalra SK, Kiran Kumar MV, Salunke P, Jaiswal AK, Jain VK. Chiari I malformation associated with atlanto-axial dislocation: focussing on the anterior cervico-medullary compression. Acta Neurochirurgica. 2007; 149: 41–50; discussion 50.

[9] Kim LJ, Rekate HL, Klopfenstein JD, Sonntag VKH. Treatment of basilar invagination associated with Chiari i malformations in the pediatric population: cervical reduction and posterior occipitocervical fusion. Journal of Neurosurgery. 2004; 101: 189–195.

[10] Liao C, Visocchi M, Zhang W, Li S, Yang M, Zhong W, *et al*. The Relationship between Basilar Invagination and Chiari Malformation Type i: a Narrative Review. Acta Neurochirurgica Supplement. 2019; 125: 111–118.

[11] Botelho RV, Heringer LC, Botelho PB, Lopes RA, Waisberg J. Posterior fossa dimensions of Chiari malformation patients compared with normal subjects: systematic review and metanalysis. World Neurosurgery. 2020; 138: 521-529.e2.

[12] Goel A. Treatment of basilar invagination by atlantoaxial joint distraction and direct lateral mass fixation. Journal of Neurosurgery: Spine. 2004; 1: 281–286.

[13] Nishikawa M, Sakamoto H, Hakuba A, Nakanishi N, Inoue Y. Pathogenesis of Chiari malformation: a morphometric study of the posterior cranial fossa. Journal of Neurosurgery. 1997; 86: 40–47.

[14] Wang S, Huang Z, Xu R, Liao Z, Yan Y, Tang W, *et al*. Chiari Malformations Type i without Basilar Invagination in Adults: Morphometric and Volumetric Analysis. World Neurosurgery. 2020; 143: e640–e647.

[15] Arnautovic A, Splavski B, Boop FA, Arnautovic KI. Pediatric and adult Chiari malformation Type i surgical series 1965-2013: a review of demographics, operative treatment, and outcomes. Journal of Neurosurgery: Pediatrics. 2015; 15: 161–177.

[16] Menezes AH. Current opinions for treatment of symptomatic hindbrain herniation or Chiari type I malformation. World Neurosurgery. 2011; 75: 226–228.

[17] Menezes AH. Craniovertebral junction abnormalities with hindbrain herniation and syringomyelia: regression of syringomyelia after removal of ventral craniovertebral junction compression. Journal of Neurosurgery. 2012; 116: 301–309.

[18] Yin Y, Yu X. Atlantoaxial facet dislocation and Chiari malformation. Journal of Neurosurgery: Spine. 2015; 23: 390–391.

[19] Roller LA, Bruce BB, Saindane AM. Demographic confounders in volumetric MRI analysis: is the posterior fossa really small in the adult Chiari 1 malformation? American Journal of Roentgenology. 2015; 204: 835–841.

[20] Ho WSC, Brockmeyer DL. Complex Chiari malformation: using craniovertebral junction metrics to guide treatment. Child's Nervous System. 2019; 35: 1847–1851.

[21] Goel A, Sathe P, Shah A. Atlantoaxial Fixation for Basilar Invagination without Obvious Atlantoaxial Instability (Group B Basilar Invagination): Outcome Analysis of 63 Surgically Treated Cases. World Neurosurgery. 2017; 99: 164–170.

[22] Frič R, Eide PK. Chiari type 1—a malformation or a syndrome? A critical review. Acta Neurochirurgica. 2019; 162: 1513–1525.

[23] Milhorat TH, Chou MW, Trinidad EM, Kula RW, Mandell M, Wolpert C, *et al*. Chiari I malformation redefined: clinical and radiographic findings for 364 symptomatic patients. Neurosurgery. 1999; 44: 1005–1017.

[24] Furtado SV, Reddy K, Hegde AS. Posterior fossa morphometry in symptomatic pediatric and adult Chiari I malformation. Journal of Clinical Neuroscience. 2009; 16: 1449–1454.

[25] Milhorat TH, Nishikawa M, Kula RW, Dlugacz YD. Mechanisms of cerebellar tonsil herniation in patients with Chiari malformations as guide to clinical management. Acta Neurochirurgica. 2010; 152: 1117–1127.
[26] Alperin N, Loftus JR, Oliu CJ, Bagci AM, Lee SH, Ertl-Wagner B, *et al*. Magnetic resonance imaging measures of posterior cranial fossa morphology and cerebrospinal fluid physiology in Chiari malformation type I. Neurosurgery. 2014; 75: 515–22; discussion 522.
[27] Tubbs RS, Hill M, Loukas M, Shoja MM, Oakes WJ. Volumetric analysis of the posterior cranial fossa in a family with four generations of the Chiari malformation Type I. Journal of Neurosurgery. Pediatrics. 2008; 1: 21–24.
[28] Frič R, Eide PK. Comparative observational study on the clinical presentation, intracranial volume measurements, and intracranial pressure scores in patients with either Chiari malformation Type I or idiopathic intracranial hypertension. Journal of Neurosurgery. 2017; 126: 1312–1322.
[29] Chandra P, Joaquim A, Tedeschi H. Controversies in the surgical management of congenital craniocervical junction disorders – a critical review. Neurology India. 2018; 66: 1003.
[30] Khalsa SSS, Siu A, DeFreitas TA, Cappuzzo JM, Myseros JS, Magge SN, *et al*. Comparison of posterior fossa volumes and clinical outcomes after decompression of Chiari malformation Type I. Journal of Neurosurgery. Pediatrics. 2017; 19: 511–517.
[31] Noudel R, Gomis P, Sotoares G, Bazin A, Pierot L, Pruvo J, *et al*. Posterior fossa volume increase after surgery for Chiari malformation Type i: a quantitative assessment using magnetic resonance imaging and correlations with the treatment response. Journal of Neurosurgery. 2011; 115: 647–658.
[32] Chou Y, Sarkar R, Osuagwu FC, Lazareff JA. Suboccipital craniotomy in the surgical treatment of Chiari I malformation. Child's Nervous System. 2009; 25: 1111–1114.
[33] Arora P, Behari S, Banerji D, Chhabra DK, Jain VK. Factors influencing the outcome in symptomatic Chiari I malformation. Neurology India. 2004; 52: 470–474.
[34] Vinchon M. Surgery for Chiari 1 malformation: the Lille experience. Child's Nervous System. 2019; 35: 1875–1880.
[35] Halvorson KG, Kellogg RT, Keachie KN, Grant GA, Muh CR, Waldau B. Morphometric Analysis of Predictors of Cervical Syrinx Formation in the Setting of Chiari i Malformation. Pediatric Neurosurgery. 2016; 51: 137–141.